Chalcogenide Letters Vol. 14, No. 8, August 2017, p. 303 - 320

SYNTHESIS AND ELASTIC PROPERTIES OF TERNARY ZnO-PbO-TeO_2 GLASSES

S. H. ALAZOUMI[a], H. A. A. SIDEK[a,*], M. K. HALIMAH[a], K. A. MATORI[a,b], M. H. M. ZAID[a,b*], A. A ABDULBASET[a]

[a]*Department of Physics, Faculty of Science, Universiti Putra Malaysia, 43400 UPM Serdang, Selangor, Malaysia*

[b]*Materials Synthesis and Characterization Laboratory, Institute of Advanced Technology, Universiti Putra Malaysia, 43400 UPM Serdang, Selangor, Malaysia*

Tellurite glass systems in the form $[ZnO]_x$ $[(TeO_2)_{0.7}\text{-}PbO)_{0.3}]_{1-x}$ (x=0, 0.15, 0.17, 0.20, 0.22 and 0.25 mol%) have been prepared by the conventional melt quenching technique. The amorphous and glassy characteristic of samples were confirmed by XRD technique. Both longitudinal and shear ultrasonic velocities were measured by using the pulse-echo method at 5 MHz resonating frequency at room temperature. Elastic moduli (longitudinal modulus, shear modulus, Young's modulus and Bulk modulus), Poisson's ratio have been calculated, and the correlation between elastic moduli with those of glass composition is discussed. All elastic constants of the glass system were estimated as well as the microhardness, acoustic impedance, thermal expansion coefficient, softening temperature, and Debye temperature has been determined using the experimental data. The experimental data of the elastic moduli for investigating glasses were compared with those of theoretically calculated values using Makishima-Mackenzie theory, bond compression model and Rocherulle model.

(Received January 16, 2017; Accepted August 11, 2017)

Keywords: Makishima-Mackenzie, Rocherulle model, Elastic moduli, Ultrasonic measurements

1. Introduction

The structure and elastic properties of glass systems are primarily influenced by the physical, chemical and electrical properties of the constituents and their compositions [1]. The strength of non-crystalline solid materials increases with their elastic moduli and hence it is possible to assess the strength indirectly from their elastic properties [2]. Studies of the elastic constant of the glassy materials give information about the structure of these non-crystalline materials, since the elastic constant are directly related to the interatomic forces and potentials [3,4,5,6], also the acoustical parameters are very informative about the microstructure as well as the behavior of the network formers and modifiers in the glass [7,8,9]. Recently, the ultrasonic pulse- echo technique has been found to be one of the best tools used for evaluating the acoustical parameters of glasses, such as elastic moduli, microhardness, Poisson's ratio, ultrasonic attenuation coefficient and Debye temperature[10,11]. Bridge et al. proposed the elastic constants of glass can be calculated by measuring the longitudinal and shear velocities of ultrasonic waves through the medium or by evaluation using the theories and semi-empirical relations [12]. They have computed the elastic moduli by considering three structural parameters: (the number of bonds per unit volume of the glass, the average cross-link density per unit glass formula and the average stretching force constant). Also, there have been several attempts to estimate elastic moduli and Poisson's ratio of glasses from packing density and dissociation energy per unit volume of chemical oxides that constituent the glass network [13,14,15,16].

* Corresponding author: mhmzaid@upm.edu.my

Among oxide glasses, TeO_2 based glasses have been attracted as gain media because of their promising properties such as high transmission from UV to IR range, low maximum phonon energy, high refractive indices, the high transmissivity of infrared radiation and excellent thermal stability and chemical durability [17,18]. TeO_2-based glasses are of scientific and technological interest such as excellent transparency in the visible and infrared regions (0.4- 6 μm), low melting temperatures, high refractive indices (~2) and high dielectric constants and electrical conductivity [19,20,21,22]. Although tremendous progress has been made. Unfortunately, there were some difficulties such as low tensile strength and strong up-conversion luminescence of tellurite glasses that have so far been hindering the tellurite glass devices for practical applications [7]. Some of these drawbacks could be overcome by adding heavy metal oxides to the glass matrix have shown better thermal stability and tensile strength[23] Besides, tellurite glasses doped with heavy metal oxides such as PbO have received significant attention because they can favourably change density, optical and thermal properties of tellurite glasses[22] .

However, adding ZnO to the lead tellurite glass lead to a change in physical and elastic properties of the lead tellurite glass. Also, the combination of the two glass modifier PbO and ZnO is an intrinsically interesting subject of study and are distinct from the properties of tellurite glass networks. Hence, the motivation of the present study is to elucidate the structural and elastic properties of ternary zinc lead tellurite glasses with varying ZnO concentration and compare the theoretical values with the experimental values of the investigated glasses.

2. Experimental Work

2.1. Preparation of glass

The $[ZnO]_x$ $[(TeO_2)_{0.7}\text{-}PbO)_{0.3}]_{1-x}$ glass system was prepared by mixing specific weights of high purity oxides, tellurium oxide, TeO_2 (Alfa Aesar, 99.99%), lead oxide, PbO (Alfa Aesar, 99.99%) and zinc oxide, ZnO (Alfa Aesar, 99.99%). The homogenization of the 15g of chemicals mixtures was effected by repeated grinding using a mortar for 30 minutes. The mixtures were preheated in an alumina crucible at 280 ºC for one hour in the electric furnace; the crucible was then transferred to the another electrical furnace for one hour at a temperature 850-900 ºC. The melt then poured into a stainless steel cylindrical shaped split mould that has been preheated. After the quenching process, the solid glass sample was annealed at 280 ºC for one hour to avoid the mechanical strain developed during the quenching process and then left to cool to room temperature[24]. The glass samples were cut into required dimension (between 6 to 10 mm) using the low-speed diamond blade to make great parallel surfaces for ultrasonic velocity measurement. Both surfaces of the samples were polished using a polishing machine with sand paper to achieve a plane parallelism.

2.2. Density and Molar volume

2.2.1. Density measurement

The density of the glass samples was measured at room temperature using a densitometer model (MD-300S Densimeter) employing the Archimedes principle using distilled water as the immersion fluid. The density resolution was estimated around $\pm$ 0.001g/cm^3. The glass samples were weighed in air, (W_{air}), and in an immersion liquid (water), (W_{water}), with (ρ_{water}=1 *g/cm*^{3}). The density of each glass samples was then measured using the following relationship:

$$\rho = \frac{W_{air}}{(W_{air} - W_{water})} \quad (1)$$

where (W_{air}) and (W_{water}) each representing the weights of the glass sample in air and distilled water, respectively.

2.2.2. Molar volume calculation

The molar volume of glass can be ideally used to describe the network structure and the arrangement of the building units since it deals directly with the spatial structure of the oxygen network[25]. Moreover, molar volume (V_m) is considered to be the better tool for studying the changes in glass structure since it eliminates mass from the density and uses an equal number of particles for comparison purposes. It is calculated from density using the equation, ($Vm=M_{glass}/\rho_{glass}$), where ($\rho_{glass}$) is the density of the glass sample and (M_{glass}) is the molecular weight of the glass. The molar volume for each glass was calculated from the relation:

$$V_m = \frac{\sum_i x_i M_i}{\rho_{glass}} \tag{2}$$

where (M_i) is molecular weight of the component oxide (i) and (x_i) is its mole fraction.

2.3. X-ray diffraction

The X-ray diffraction (XRD) system was used to determine the amorphous nature of the samples using X'Pert Pro Panalytical PW 3040 MPD X-ray powder diffraction instrument in the range of (2θ) from 4° to 90°.

2.4. Ultrasonic velocity measurements

Ultrasonic velocity measurements were carried out at room temperature and 5 MHz in both shear and longitudinal modes by employing ultrasonic pulse-echo technique by RITEC RAM-5000 Snap System. Ultrasonic velocity is calculated using the following equation:

$$V = \frac{2X}{t} \quad (ms^{-1}) \tag{3}$$

where X is, the thickness of the sample, V is the velocity, and t is the transit time.

2.5. The elastic properties

The elastic properties of the $[ZnO]_x\ [(TeO_2)_{0.7}\text{-}PbO)_{0.3}]_{1\text{-}x}$ glasses with different percentage of x, such as, the longitudinal modulus L, the shear modulus G, the bulk modulus K, Young's modulus E, and Poisson's ratio σ have been calculated using the measured ultrasonic velocities and density from the following equations:

$$\text{Longitudinal modulus } (L) = V_L^2 \rho \tag{4}$$

$$\text{Shear modulus } (G) = V_S^2 \rho \tag{5}$$

$$\text{Bulk modulus } (K) = L - \left(\frac{4}{3}\right) G \tag{6}$$

$$\text{Young's Modulus } (E) = 2G(1+\sigma) \tag{7}$$

$$\text{Poisson's ratio } (\sigma) = \left(\frac{L-2G}{2(L-G)}\right) \tag{8}$$

where (V_L) and (V_S) are longitudinal and transverse velocities, respectively. Besides, the fractal bond connectivity (d), the microhardness (H), acoustic impedance (Z), thermal expansion coefficient (α_P), Debye temperature (θ_D), and Softening temperature (T_S) are given by the following equations:

$$d = \frac{4G}{K} \tag{9}$$

$$H = \frac{(1-2\sigma)E}{6(1+\sigma)} \tag{10}$$

$$Z = \rho V_L \tag{11}$$

$$\alpha_P = 23.2(V_L - 0.57457) \tag{12}$$

$$\theta_D = \left(\frac{h}{K_B}\right)\left(\frac{3PN_A}{4\pi V_m}\right)^{\frac{1}{3}} U_m \tag{13}$$

$$T_S = \frac{MV_S^2}{PC^2} \tag{14}$$

where (h) is Plank's constant, (K_B) is Boltzmann's constant, (U_m) is the mean ultrasonic velocity, (N_A) is Avogadro's number, (V_m) is the molar volume calculated from the effective molecular mass and the density (M/ρ), and (P) is the number of atoms in the chemical formula and (C) is the constant of proportionality and has the value 507.4 ($ms^{-1}K^{-1/2}$). The mean ultrasonic velocity, (U_m) is equal to:

$$U_m = \left(\frac{1}{3}\right)\left(\frac{1}{V_L^3} + \frac{2}{V_S^3}\right)^{-\frac{1}{3}} \tag{15}$$

3. Theoretical models

3.1. Bond compression model

the bond compression model [12] is a helpful introduce for structures containing only on type of bond. For a three-dimensional multi- component oxide glass, the bulk modulus (K_{bc}) is given by the equation:

$$K_{bc} = \frac{n_b \bar{F} r^2}{9} \tag{16}$$

where $(\bar{F})$ is the average stretching force constant, r is the bond length between cation and anion and (n_b) is the number of network bond per unit volume of the glass is given by

$$n_b = \frac{\rho N_A}{M} \sum_i (x n_f)_i \tag{17}$$

However, for polycomponent glasses with (i) different types of network bonds, Equation (16) and Equation. (17) can be written as

$$K_{bc} = (\rho N_A / 9M) \sum_i (x n_f \bar{F} r^2)_i \tag{18}$$

where (x) is the mole fraction of the component oxide (i), (n_f) is the number of network bonds per glass formula unit, while (N_A), ρ and (M) are Avogadro's number, density and molecular weight of the glass, respectively.

Where $(\bar{F})$ is the average of stretching force constant and can be calculated from following equation:

$$\bar{F} = \frac{\sum_i (x n_f F)_i}{\sum_i (x n_f)_i} \tag{19}$$

where (n_f) is the coordination number of the cation and (F) is the stretching force constant of the oxide.

The calculated Poisson's ratio (σ_{bc}) and the average crosslink density ($\overline{n_c}$) were calculated by using the following Equation [26]

$$\sigma_{bc} = 0.28(\overline{n_c})^{-0.25} \tag{20}$$

Where ($\overline{n}_c$) is the number of cross-links per glass formula is given as

$$\bar{n}_c = \frac{1}{\eta}\sum_i (x n_c N_c)_i \tag{21}$$

where (n_c) is the number of cross-link per cation (number of bridging bonds per cation minus 2) in oxide (i). (N_c) is the number of cation per glass formula unit and (η) is the total number of cations per glass formula unit and can be calculated from the equation

$$\eta = \sum_i (x N_c)_i \tag{22}$$

A quantitative interpretation of the experimental elastic behaviour based on the ring deformation model of the bulk modulus is attempted [27]. According to this model, bulk modulus is expressed in the form:

$$K_e = 0.0106 \bar{F} (l)^{-3.84} \tag{23}$$

where (l) is the external ring diameter defined as ring perimeter (number of bonds in ring multiplied by bond length) divided by (π).

After calculating both (K_{bc}) and (σ_{bc}) the rest of the elastic moduli for each glass system can be calculated as follows:

$$G_{bc} = (3/2) K_{bc} \left(\frac{1-2\sigma_{bc}}{1+\sigma_{bc}}\right) \tag{24}$$

$$L_{bc} = K_{bc} + (4/3) G_{bc} \tag{25}$$

$$E_{bc} = 2G(1 + \sigma_{bc}) \tag{26}$$

The ratio (K_{bc}/K_e), where (K_e) is an experimental value, is a measure of the extent to which bond bending is governed by the configuration of the network bonds, that is, (K_{bc}/K_e) is assumed to increase with average atomic ring size (l). The average atomic ring size is expressed according to the equation,

$$l = \left(0.0106 \frac{\bar{F}}{K_e}\right)^{0.26} \tag{27}$$

Where $\bar{F}$ isthe average stretching force constant.

3.2. Makishima and Mackenzie model

Makishima and Mackenzie [13], [14] proposed a theoretical model for the direct calculation of Young's modulus of oxide glasses regarding their chemical compositions taking into consideration the two parameters; dissociation energy of the oxide constituents per unit volume (G_t) and packing density of glasses (V_t). The elastic moduli and Poisson's was given as,

Young's modulus in a single-component glass, $E_m = 2V_t G_t$ (28)

For polycomponent glasses, $E_m = 2V_t \sum_i G_i x_i$ (29)

The packing density, V_t is defined by $V_t = \left(\frac{\rho}{M}\right) \sum_i V_i x_i$ (30)

Bulk modulus, $K_m = 1.2 V_t E$ (31)

$$\text{Shear modulus, } G_m = (3EK/9K - E) \tag{32}$$

$$\text{Poisson's ratio, } \sigma_m = (E/2G_m - 1) \tag{33}$$

where (M) is the effective molecular weight, ρ is the density, x_i is the mole fraction component (i), and (Vt) is a packing factor obtained from the following equation for oxide ($A_x\ O_y$):

$$V_i = N_A(4\pi/3)(xR_A^3 + yR_O^3) \tag{34}$$

where (R_A) and (R_O) are the respective ionic radius of metal and oxygen (Pauling's ionic radii).

3.3. Rocherulle model

Rocherulle et al. [15] introduced some modifications in the expression of packing factor, which has been proposed by Makishima and Mackenzie [13,14] for oxides, and reported the following relations for calculating packing density, (Ci) defined as follows:

$$C_i = N_A(4\pi\rho/3M)(xR_A^3 + yR_O^3) \tag{35}$$

For a polycomponent glass, the (C_t) factor will, therefore, be expressed as follows:

$$C_t = \sum_i C_i x_i \tag{36}$$

$$C_t = \sum_i \frac{\rho_i}{M_i} V_i x_i \tag{37}$$

4. Results and discussion

4.1. Density and Molar volume

Density and calculated molar volume values are reported in Table 1. It has been observed that both values decrease with increasing content of transition metal oxide ZnO in glass system. Fig. 1 shows the variation of density and molar volume for studied glasses as a function of ZnO content (mol%). The measured densities of the glasses are high as listed in Table 1; it can be seen that the density decreases gradually as the weight fraction of ZnO. The replacement of ZnO (with lower molecular weight 81.38 *g/mol*) at the expense of TeO_2 and PbO (with higher molecular weights 159.598 and 223.1994 *g/mol*, respectively), leads to decrease in density from 6.257 to (6.078 *g* cm^{-3}) with the increase of ZnO content from 15 to 25 mol%. The molar volume decreases from 26.22 to 25.40 cm^3/mol with the increase in the concentration of ZnO,

The glass structure can be explained regarding molar volume rather than density, as the former deals the spatial distribution of the ions forming that structure. The change in the molar volume with the molar composition of an oxide indicates the preceding structural changes through a formation or modification process in the glass network[28].The decrease in molar volumes with an increase in densities as presented in Table 1 is due to the rearrangement of the lattice and a reduction in the porosity of the glass. The decreases in molar volumes for this ternary glass system which range from 26.22 to 25.40 (cm^3/mol) attributed to a reduction in the bond length or interatomic spacing between the atoms. Finally, it is important to note that the small variation of the densities and molar volume is due to the low change in concentration of ZnO.

Table 1: Experimental values of density (ρ), molar volume (V_m), longitudinal (V_L), shear (V_S) and Mean (U_m) ultrasonic wave velocity of ternary $[ZnO]_x [(TeO_2)_{0.7}\text{-}PbO)_{0.3}]_{1-x}$ glass system.

x (*mol %*)	Density ρ (kgm^{-3})	Molar Volume V_m ($cm^3.mol^{-1}$)	Longitudinal V_L ($m.s^{-1}$)	Shear V_S	Mean velocity U_m
15	6257	26.22	2743.32	1551.16	1725.15
17	6230	26.03	2776.99	1590.00	1766.48
20	6191	25.72	2795.97	1606.15	1783.92
22	6144	25.60	2865.07	1655.17	1837.45
25	6078	25.40	2885.42	1669.57	1853.18

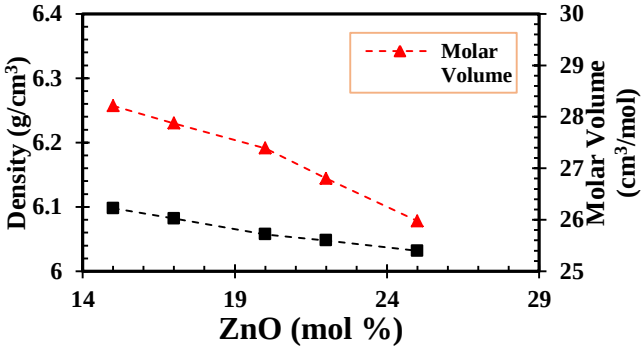

Fig. 1. Density (ρ) and molar volume (V_m) of the $[ZnO]_x [(TeO_2)_{0.7}\text{-}PbO)_{0.3}]_{1-x}$ glasses.

4.2. X-ray diffraction

XRD patterns for all the $[ZnO]_x [(TeO_2)_{0.7}\text{-}PbO)_{0.3}]_{1-x}$; x=15, 17,20,22 and 25 mol % glass samples were observed to have no sharp peaks which confirm the amorphous nature of the prepared glasses as seen in Fig. 2.

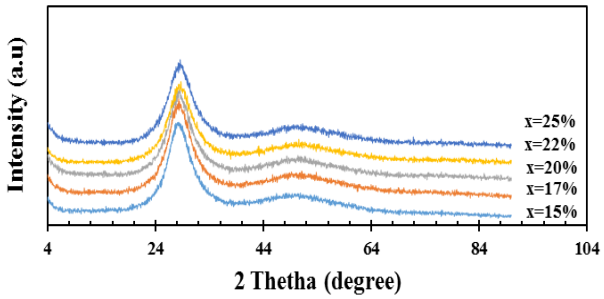

Fig. 2. XRD patterns of $[ZnO]_x [(TeO_2)_{0.7}\text{-}PbO)_{0.3}]_{1-x}$ glasses.

4.3. Ultrasonic measurements

4.3.1. Ultrasonic velocities

The variation of ultrasonic velocities, in TeO_2–PbO–ZnO glasses at room temperature, as a function of PbO mol% content is shown in Fig. 3. Table 2 shows both longitudinal and shear ultrasonic velocities increase from 2743.32 and 1551.16 (*m/s*) to 2885.42 and 1669.57 (*m/s*) for longitudinal and shear velocities respectively as the zinc oxide content increases. The increment in velocities can be attributed mainly to the increase in rigidity and elastic properties of the glass.

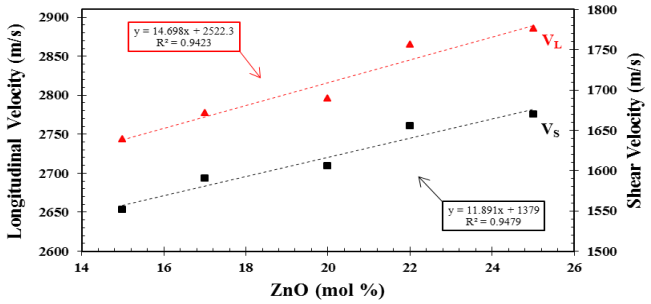

Fig. 3. Ultrasonic velocities (Longitudinal (V_L) and shear (V_S) of$[(TeO_2)_{0.7}\text{-}PbO)_{0.3}]_{X\text{-}1}[ZnO]_X$ glasses.

4.4. Elastic moduli, Poison's ratio, (*E/G*) ratio and Fractal bond connectivity:

The calculated values of the longitudinal modulus (*L*), shear modulus (*G*), bulk modulus (*K*), Young's modulus (*E*), (*E/G*) ratio and Poisson's ratio (σ) of the samples are listed in Table 2. The results show that the elastic moduli increase with increasing (ZnO) mole percentage content from 15 to 25. Longitudinal modulus ranged from 47.09 to 50.61 (*GPa*), shear modulus from 15.05 to 16.94 (*GPa*), Young's modulus from 38.09 to 42.30 (*GPa*), and bulk modulus from 27.01to 28.01 (*GPa*) have been observed. Fig. 4. shows the variation of elastic moduli data of lead tellurite glass with different values of (ZnO) mole percent; it is evident that the elastic moduli values are gradual increases with the different percentage of (ZnO) mol%. The addition of zinc oxide to the $[(TeO_2)_{0.7}\text{-}PbO)_{0.3}]_{X\text{-}1}[ZnO]_X$ network increases both ultrasonic velocities and this, in turn, leads to increasing the rigidity of glass and hence to an increase in elastic moduli.

Fig. 5 shows the variation of Poison's ratio (σ) and (*E/G*) ratio; it is clear that the behaviour of (σ) is similar to that of (*E/G*) ratio with a variation of the content (ZnO) mol%. Moreover, the decrease in Poisson's ratio (σ) in this glass system means the reduction in the ratio of lateral to longitudinal strains confirming the increase in the linkages between (Te–O) chains.

Dimensionality of the amorphous structure can be described with an important parameter related to the elasticity's constants; It called the d ratio which equals to (4 *G/K*).The value of d is 3 for 3D networks of tetrahedral coordination polyhedral, 2 for 2D layer structures and 1 for 1D chain[29]. It is apparent from Table 3 and fig 6. that, the values of fractal bond connectivity of these glasses increase from 2.23 to 2.42. It is close to 2, which indicates that the network of these glasses has 2D layer structure.

Table 2: Experimental values of elastic moduli, Poison's ratio (σ) and (E/G) ratio of ternary $[ZnO]_x$ $[(TeO_2)_{0.7}\text{-}PbO)_{0.3}]_{1\text{-}x}$ glass system.

X	Elastic Constants (*GPa*)				Poisson's ratio	(*E/G*)
(*mol %*)	*L*	*G*	*K*	*E*	(σ)	ratio
15	47.09	15.05	27.01	38.09	0.2650	2.530
17	48.04	15.75	27.04	39.57	0.2561	2.512
20	48.40	15.97	27.10	40.05	0.2537	2.507
22	50.43	16.83	27.99	42.06	0.2495	2.499
25	50.61	16.94	28.01	42.30	0.2483	2.496

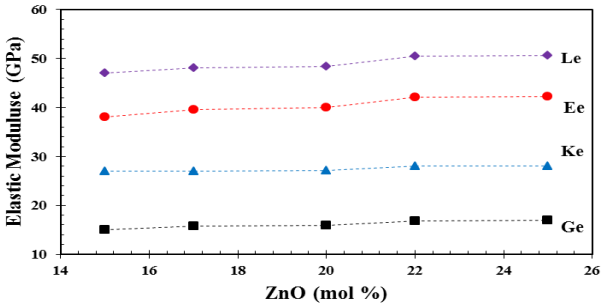

Fig. 4. Elastic moduli longitudinal (L), shear (G), bulk modulus (K) and Young's (E) vs. the mole percentage of (ZnO) for $[ZnO]_x\,[(TeO_2)_{0.7}\text{-}PbO)_{0.3}]_{1\text{-}x}$ *tellurite glasses.*

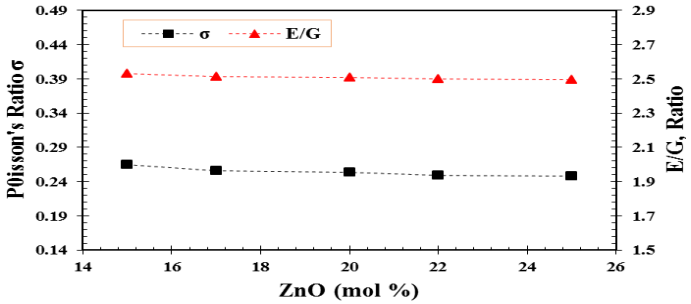

Fig. 5. Variation of Poison's and (E/G) ratio for glass samples with different mol% of (ZnO).

4.5. Characteristic Temperatures and Microhardness

The Debye temperature (θ_D) is an important parameter of solids; it represents the temperature at which nearly all the vibration modes are excited. The softening temperature (T_S), is another important parameter defined as the temperature at which viscous flow changes to plastic flow[30]. The two temperatures can be calculated according to the relations;(13) and (14) respectively. Debye temperature and the softening temperature are illustrated in Table 3 and Fig. 7. It can be observed that both the Debye and softening temperatures increased from 200.22 and 590.94 *K* to 215.42 and 661.85*K*, respectively, as the content of ZnO. The increase in the mean ultrasonic velocity (U_m) and consequently the increase in Debye and softening temperatures are mainly due to the decrease in the number of NBOs as a direct effect of the insertion of ZnO.

The present study of increasing trend of the thermal coefficient (αp) reveals an increasing number of bonds per unit volume and account for enhancement of rigidity of glass structure in the glass specimen. The thermal expansion coefficient (αp) increase with (ZnO) content. It was found to increase from 63631.72to 66928.50 (K^{-1}) as shown in Table 3.

Microhardness expresses the required stress to eliminate the free volume (deformation of the network) of the glass. The microhardness (*H*) was calculated from Young's modulus (*E*) and Poisson's ratio (σ) according to the relationship (11). The increase in the microhardness indicates the increase in the rigidity of the glass. The microhardness as shown in Fig. 6 increases as Poisson's ratio decreases. Table 3 presents the calculated values of microhardness (*H*), It can be seen that microhardness increased from 2.36 (*GPa*) to 2.84 (*GPa*) with increasing (ZnO).

Table 3. Microhardness (H), Debye temperature (θ_D), softening temperature (T_S), Thermal expansion coefficient (α_P), fractal bond connectivity (d) and acoustic impedance (Z) of ternary $[ZnO]_x [(TeO_2)_{0.7}PbO)_{0.3}]_{1-x}$ glass system.

x (*mol %*)	T_S (*K*)	θ_D (*K*)	H (*GPa*)	α_P (K^{-1})	d	$Z\times10^{-7}$ ($Kg.m^{-2}.s^{-1}$)
15	590.94	200.22	2.36	63631.72	2.23	1.716
17	616.87	205.17	2.56	64412.77	2.33	1.730
20	623.20	207.45	2.62	64853.07	2.36	1.731
22	657.32	213.62	2.81	66456.31	2.41	1.760
25	661.85	215.42	2.84	66928.50	2.42	1.754

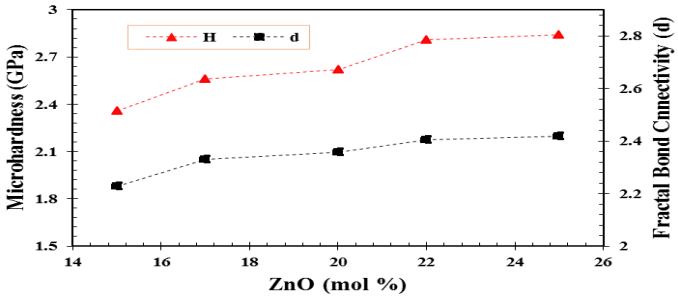

Fig. 6. Microhardness (H) and fractal bond connectivity (d) of ternary $[ZnO]_x [(TeO_2)_{0.7}PbO)_{0.3}]_{1-x}$ glass system.

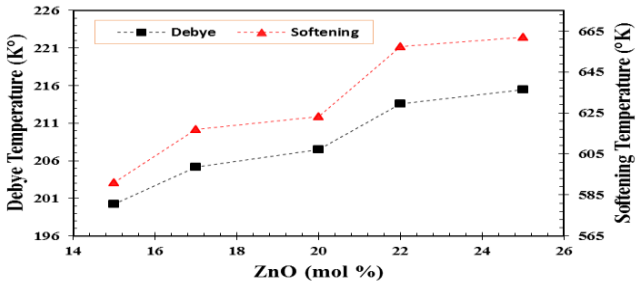

Fig. 7. Variation of Debye and softening temperature for glass samples with different mol% of ZnO.

4.5. Theoretical Elasticity Models

4.5.1. Bond compression model

The model assumes that the elastic moduli depend on the number of bonds per cation and the average force constants. Also, the ratio between the calculated elastic moduli and the experimental one (K_{bc}/K_e) is assumed to be directly proportional to the atomic ring size (l)[31].Table 4 gives values of the constants used in the calculations of the equations derived from the bond compression model. It presented the values of the coordination number (n_f), crosslink density per cation (n_c), cation–anion bond length (r), and stretching force constant (F) of TeO_2, PbO and ZnO oxides. Table 5 gives values of the number of network bonds per unit volume (n_b), the average cross-link density ($\overline{n}_c$), the experimentally determined bulk modulus (K_e), the bond compression bulk modulus(K_{bc}), the ratio(K_{bc}/K_e), the average force constant F and the average ring diameter (l). It is quite clear from Table 5 that the bulk modulus K_{bc} increases from 110.31to

111.24 GPa with the increase of ZnO content from 15 to 25 mol%. This increase in (K_{bc}) is expected since (K_{bc}) depends on the number of network bonds per unit volume (n_b). Moreover, the number of network bonds per unit volume increases from 9.87×10^{28} to 10.67×10^{28} m^{-3}, the stretching force constant decreases from 160.17 to 140.77 $N.m^{-1}$ with the increase of ZnO content from 15 to 25 mol% as shown in Fig. 8. Furthermore, values of the ratio (K_{bc}/K_e) ranges between 4.08 and 3.97 as shown in Fig. 9. It is evident from the Figure that (K_{bc}/K_e) decreases gradually as the ZnO oxide concentration increases. The ring size ranges between 0.487 to 0.467 *nm*. Dependence of the ratio (*Kbc/Ke*) on the ring diameter demonstrated in Figure 10.

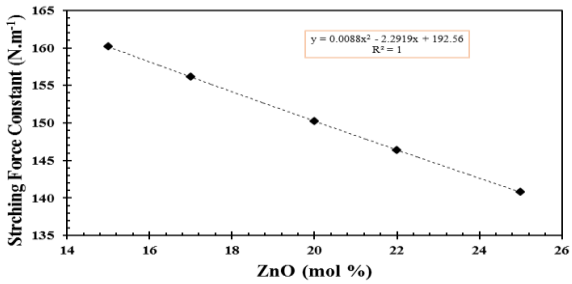

Fig.8. Variation of stretching force constant with ZnO (mol%) content.

Table 4: Coordination number (n_f), cation–anion bond length r (nm), crosslink density per cation (n_c) and Stretching force constant of the oxide F($N.m^{-1}$) of (TeO_2) , (PbO) and (ZnO) oxides [32].

Oxide	(n_f)	n_c	*r* (*nm*)	*F* ($N.m^{-1}$)
TeO_2	4	2	0.199	216
PbO	4	2	0.230	139
ZnO	6	4	0.1988	219

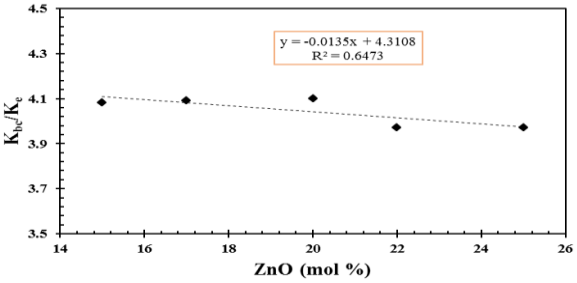

Fig.9. Variation of the ratio (K_{bc}/K_e) of the glass system $[ZnO]_x\,[(TeO_2)_{0.7}\text{-}PbO)_{0.3}]_{1-x}$ with the mol% of the ZnO.

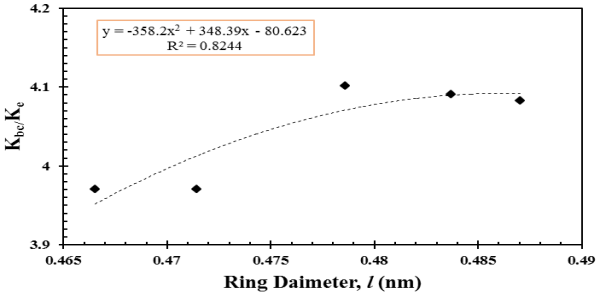

Fig.10. Dependence of the ratio (K_{bc}/K_e) on the ring diameter of the glass system $[ZnO]_x\,[(TeO_2)_{0.7}\text{-}PbO)_{0.3}]_{1-x}$.

Table 5. The number of network bonds per unit volume (n_b), the average cross-link density ($\overline{n}_c$), the experimentally determined bulk modulus (K_e), the bond compression bulk modulus (K_{bc}), the ratio (K_{bc}/K_e), the average force constant ($\overline{F}$), the average ring diameter (l) of $[ZnO]_x [(TeO_2)_{0.7}\text{-}PbO)_{0.3}]_{1-x}$ glasses.

x(mol%)	$n_b \times 10^{28}$(m^{-3})	K_{bc} (GPa)	K_{bc}/K_e	$\overline{F}$ ($N.m^{-1}$)	($\overline{n}_c$)	l (nm)
15	9.87	110.31	4.08	160.17	2.30	0.487
17	10.04	110.63	4.09	156.142	2.34	0.484
20	10.30	111.16	4.10	150.25	2.40	0.479
22	10.45	111.15	3.97	146.40	2.44	0.471
25	10.67	111.24	3.97	140.77	2.50	0.467

4.6. Makishima–Mackenzie model

Makishima–Mackenzie suggested that the elastic module is the function of both the packing density (ionic radii of elements) and the average strength (dissociation energy) of the chemical bonds in the glass. Table 6 presents packing factor and dissociation energy per unit volume of (TeO_2), (PbO) and (ZnO) oxides. The values of the packing factors and dissociation energy per unit volume for (TeO_2) are 14.7 $cm^3\ mol^{-1}$ and 54 $kJ.cm^{-3}$,(ZnO) are 7.9 $cm^3\ mol^{-1}$ and 49.9 $kJ.cm^{-3}$ [33] respectively. While the values for (PbO) are 11.7 $cm^3\ mol^{-1}$ and 17.55 $kJ.cm^{-3}$ [15] respectively. Table 7 presents molecular weight (M_i), Dissociation energy per unit volume(G_t), packing density (V_t), packing factor (C_t) and elastic module and Poison's ratio (σ_m) calculated according to Makishima–Mackenzie mode of $[ZnO]_x [(TeO_2)_{0.7}\text{-}PbO)_{0.3}]_{1-x}$ glasses. The evaluation of the elastic moduli according to Makishima–Mackenzie model of the glasses studied is given in Table 7. The results reveal that the values of the elastic moduli are lower than those measured experimentally. The addition of (ZnO) will decrease the packing density (V_t) from 0.4925 to 0.4853 as shown in Fig.11. On the contrary, the Dissociation energy per unit volume (G_t) and packing factor (C_t) decreases with the increase in (ZnO) content, as dissociation energy per unit volume of (ZnO) is lower than the dissociation energy per unit volume of (TeO_2); since dissociation energy per unit volume (ZnO) is 49.9 $kJ.cm^{-3}$ to dissociation energy for (TeO_2) is 54 $J.cm^{-3}$. Also, the addition of (ZnO) content from 15 up to 25 mol % will result in a slight decrease in shear (G_m), Young's (E_m) and bulk (K_m) elastic module and calculated Poison's ratio (σ_m) as shown in Table. 7 .

Table 6: Packing factor and dissociation energy per unit volume of (TeO_2), (PbO) and (ZnO) oxides.

oxide	V_i ($cm^3\ mol^{-1}$)	G_i ($KJ.cm^{-3}$)	(Reference)
TeO2	14.7	54	[33]
PbO	11.7	17.55	[15]
ZnO	7.9	49.9	[33]

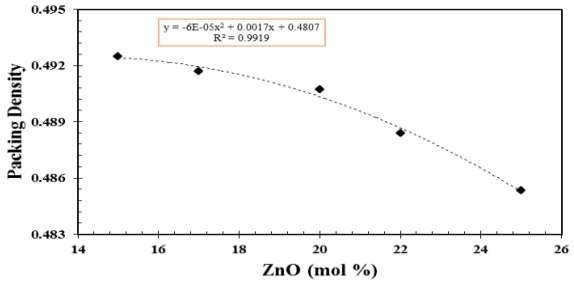

Fig. 11. Dependence of the packing density of ternary glass system $[ZnO]_x [(TeO_2)_{0.7}\text{-}PbO)_{0.3}]_{1-x}$ on the percentage of the modified ZnO.

Table 7: Molecular weight (M_i), Dissociation energy per unit volume (G_t), packing density (V_t) , packing factor (C_t) and elastic moduli (E_m, G_m, K_m) calculated Poison's ratio (σ_m) according to Makishima–Mackenzie mode of $[(TeO_2)_{0.7}\text{-}PbO)_{0.3}]_{X\text{-}1}[ZnO]_X$ glasses.

x_i (*mol %*)	M_i ($g.mol^{-1}$)	V_t	C_t	G_t (10^9 J/m^3)	E_m (*GPa*)	G_m (*GPa*)	K_m (*GPa*)	σ_m
15	164.08	0.4925	0.5197	42.8430	42.20	17.323	24.939	0.2179
17	162.14	0.4917	0.5203	42.8114	42.10	17.290	24.842	0.2175
20	159.22	0.4907	0.5212	42.7640	41.97	17.244	24.714	0.2169
22	157.27	0.4884	0.5218	42.7324	41.74	17.169	24.464	0.2156
25	154.35	0.4853	0.5226	42.6850	41.43	17.067	24.129	0.2138

4.7. Rocherulle model

The calculated values of the elastic moduli and Poisson's ratio from the Rocherulle et al.[15] model for the studied glass system is given in Table 8. It can be seen that the elastic moduli increase with increasing (ZnO) mole percentage content from 15 to 25. The increment in Shear modulus from 18.062 to 18.074 *GPa*, Young's modulus from 44.54 to 44.62 *GPa*, and bulk modulus from 27.78 to 27.98 *GPa* has been observed. The result of experimental elastic moduli (Young's modulus, shear modulus and bulk modulus) and Poisson's ratio of $[ZnO]_x$ $[(TeO_2)_{0.7}\text{-}PbO)_{0.3}]_{1\text{-}x}$ glasses are compared with the theoretically calculated value from Rocherulle's model as shown in Table 9. A good percentage of coincidence have been observed between the theoretically calculated and experimentally measured values of elastic moduli and Poisson's ratio of glasses. The addition of (ZnO) will increase Packing factor (C_t) from 0.5197 to 0.5226 as shown in Fig 12 and Table 8.

Table 8: Packing factor (C_t), Calculated elastic moduli (E_r, G_r, K_r) and Poisson's ratio (σ_r) for $[ZnO]_x$ $[(TeO_2)_{0.7}\text{-}PbO)_{0.3}]_{1\text{-}x}$ glass system from the model of Rocherulle et al model.

x_i (*mol %*)	C_t	*Er* (*GPa*)	*Gr* (*GPa*)	*Kr* (*GPa*)	σ_r
15	0.5197	44.54	18.062	27.78	0.2328
17	0.5203	44.55	18.065	27.82	0.2330
20	0.5212	44.57	18.069	27.88	0.2335
22	0.5218	44.59	18.071	27.92	0.2338
25	0.5226	44.62	18.074	27.98	0.2343

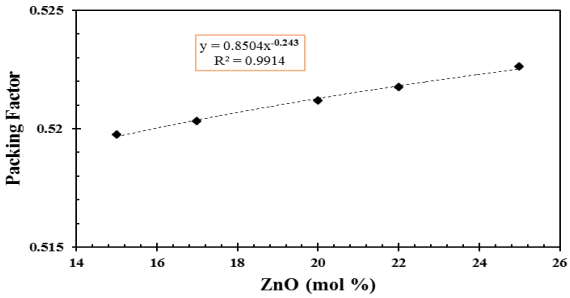

Fig.12. Dependence of the packing factor of ternary glass system $[ZnO]_x\ [(TeO_2)_{0.7}\text{-}PbO)_{0.3}]_{1-x}$ on the percentage of the modified ZnO.

4.8. Agreement between experimental and theoretical elastic moduli and Poisson's ratio

Table 9 summarises the results of the experimental elastic module and those of calculated from the bond compression, Makishima–Mackenzie and Rocherulle models for ternary tellurite glasses $[ZnO]_x\ [(TeO_2)_{0.7}\text{-}PbO)_{0.3}]_{1-x}$. The result shows a fairly good agreement between the observed and the calculated values of Poisson's ratio. Also, it can be seen the good agreement values between the observed and theoretically calculated values of shear and Young's modulus are valid for the Makishima–Mackenzie and Rocherulle models. Dependence of elastic modulus on (ZnO) (*mol %*) concentration in $[ZnO]_x\ [(TeO_2)_{0.7}\text{-}PbO)_{0.3}]_{1-x}$ glass demonstrated in Fig. 13, 14 and 15. It can be seen clearly from Figure 13 that, the theoretical values of bulk modulus (K_e, K_m, K_{bc} and K_r) from Makishima–Mackenzie model are smaller than the corresponding experimental values. While the calculated value of (K_{bc}) is higher than that obtained experimentally (K_e) as shown in Table 9. It was stated that (K_{bc}) is always greater than the experimental value, typically by a factor of 3–10, and the ratio (K_{bc}/K_e) forms a rough measure of the degree to which bond bending process are involved in isotropic elastic deformation of the structure[34].

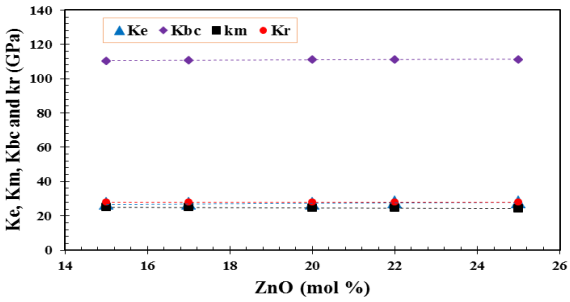

Fig.13. Dependence of bulk modulus (K_e, K_m, K_{bc} and K_r) on (ZnO) (mol %) concentration in $[ZnO]_x\ [(TeO_2)_{0.7}\text{-}PbO)_{0.3}]_{1-x}$ glass.

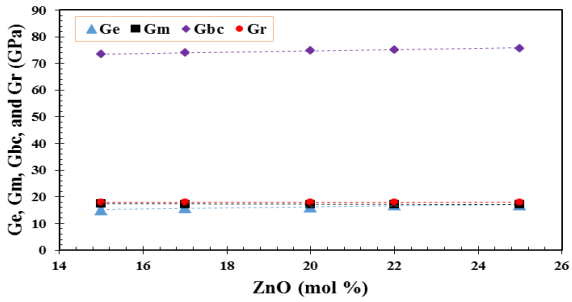

Fig. 14. Dependence of shear modulus (G_e, G_m, G_{bc} and G_r) on (ZnO) (mol %) concentration in $[ZnO]_x [(TeO_2)_{0.7}\text{-}PbO)_{0.3}]_{1-x}$ glass.

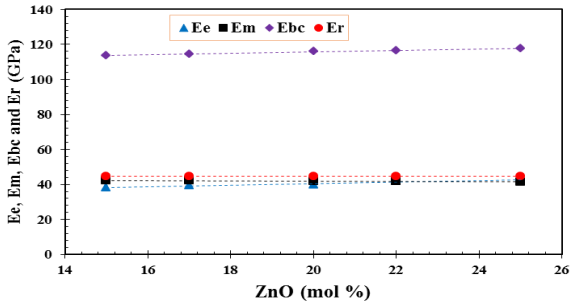

Fig.15. Dependence of Young's modulus (E_e, E_m, E_{bc} and E_r) on (ZnO) (mol %) concentration in $[ZnO]_x [(TeO_2)_{0.7}\text{-}PbO)_{0.3}]_{1-x}$ glass.

Table 9: Experimental elastic moduli (E_e, G_e, K_e), bond compression model (E_{bc}, G_{bc},K_{bc}), Rocherulle model (E_r, G_r, K_r)and Makishima and Mackenzie model (E_m, G_m, K_m) for Young's, shear and bulk modulus, respectively and Poisson's ratio (σ_e, σ_{bc} ,σ_r, σ_m) of binary $[(TeO_2)_{0.7}\text{-}PbO)_{0.3}]_{X\text{-}1}[ZnO]_X$ glass system.

x	$E(GPa)$				$G(GPa)$				$K(GPa)$				Σ			
(*mol%*)	E_e	E_r	E_m	E_{bc}	G_e	G_r	G_m	G_{bc}	K_e	K_r	K_m	*Kbc*	σ_e	σ_r	σ_m	σ_{bc}
15	38.09	44.54	42.20	113.59	15.05	18.062	17.323	73.51	27.01	27.78	24.939	110.31	0.2650	0.2328	0.2179	0.2274
17	39.57	44.55	42.10	114.56	15.75	18.065	17.290	74.04	27.04	27.82	24.842	110.63	0.2561	0.2330	0.2175	0.2263
20	40.05	44.57	41.97	116.06	15.97	18.069	17.244	74.88	27.10	27.88	24.714	111.16	0.2537	0.2335	0.2169	0.2249
22	42.06	44.59	41.74	116.67	16.83	18.071	17.169	75.18	27.99	27.92	24.464	111.15	0.2495	0.2338	0.2156	0.2240
25	42.30	44.62	41.43	117.67	16.94	18.074	17.067	75.69	28.01	27.98	24.129	111.24	0.2483	0.2343	0.2138	0.2226

5. Conclusion

Ternary tellurite glasses with composition $[ZnO]_x\ [(TeO_2)_{0.7}\text{-}PbO)_{0.3}]_{1\text{-}x}$, x = 0.15, 0.17, 0.20, 0.22 and 0.25 mol, has been successfully prepared. XRD patterns show that the present glasses were amorphous in nature. The density and molar volume of zinc lead tellurite glasses decrease as ZnO content increases. Ultrasonic velocities, elastic moduli, Debye temperature, softening temperature, microhardness, thermal expansion coefficient, fractal bond connectivity and acoustic impedance increase with an increase in the ZnO content, which is attributed to the increase in rigidity and the connectivity of the network structure.

As the content of ZnO increases, the average ring diameter and the ratio (K_{bc}/K_e) decreases, while the number of bonds per unit volume increases. This ascribed to the increase of the increase of the rigidity of the glass structure.

Comparison of theoretical and experimental values of elastic moduli and Poisson's ratio of the $[ZnO]_x\ [(TeO_2)_{0.7}\text{-}PbO)_{0.3}]_{1\text{-}x}$ glass system leads to the conclusions that:

1. The correlation between the observed and theoretically calculated values of shear and Young's modulus from the Makishima – Mackenzie model is satisfactory.
2. The excellent agreement between the observed and theoretically calculated values of the bulk modulus and Poisson's ratio were identified for the Rocherulle model.
3. The bond compression model is not suitable for these glasses because Young's modulus, shear modulus and bulk modulus are not comparable with those of experimental data.

Acknowledgements

The researchers gratefully acknowledge the financial support for this study from the Malaysian Ministry of Higher Education (MOHE) and Universiti Putra Malaysia through the Fundamental Research Grant Scheme (FRGS) and Inisiatif Putra Berkumpulan (IPB) research grant.

References

[1] K. T. Arulmozhi, R. Sheelarani, Journal of Non-Crystalline Solids **357(**16–17), 3272 (2011).
[2] M. H. M. Zaid, K. A Matori, L. C. Wah, H. A A Sidek, M. K. Halimah, Z. A Wahab, B. Z. Azmi, International Journal of the Physical Sciences, **6(**6), 1404 (2011).
[3] Y. Zhou, Y. Yang, F. Huang, J. Ren, S. Yuan, G. Chen, Journal of Non-Crystalline Solids, **386**, 90 (2014).
[4] H. A. A. Sidek, S. Rosmawati, Z. A. Talib, M. K. Halimah, S. A. Halim, International Journal of Basic & Applied Sciences, **90**, 41 (2013).
[5] C. Bootjomchai, R. Laopaiboon, S. Pencharee, J. Laopaiboon, Journal of Non-Crystalline Solids **388**, 37 (2014).
[6] N. S. A. B. D. El-aal, H. A. Afifi, Archives of Acoustics, **654**(4), 641 (2009).
[7] M. K. Halimah, W. M. Daud, H. A. A. Sidek, Chalcogenide Letters, **7(**11), 613 (2010).
[8] H. A. A. Sidek, R. El-Mallawany, K. Hariharan, S. Rosmawati, Advances in Condensed Matter Physics, vol. 2014, 2014.
[9] A. A. El-Moneim, Physica B: Condensed Matter, **487**, 53 (2016).
[10] A. Abd El-Moneim, Journal of Non-Crystalline Solids, **405**, 141 (2014).
[11] A. Abd El-Moneim, Materials Chemistry and Physics **135**(2–3), 653 (2012).
[12] B. Bridge, "On the Elastic Constants and Structure BY," vol. 655, 1983.
[13] A. Makishima, J. D. Mackenzie, Journal of Non-Crystalline Solids, **12(**1), 35 (1973).
[14] A. Makishima, J. D. Mackenzie, Journal of Non-Crystalline Solids, **17(**2), 147 (1975).
[15] J. Rocherulle, C. Ecolivet, M. Poulain, P. Verdier, Y. Laurent, Journal of Non-Crystalline Solids **108(**2), 187 (1989).
[16] A. Abd El-Moneim, M. D. Alenezy, "Structural and acoustical properties of lead silicate glasses doped with alkali and alkaline earth oxides," no. October 2013, 2016.

[17] Y. Wang, S. Dai, F. Chen, T. Xu, Q. Nie, Materials Chemistry and Physics **113**(1), 407 (2009).
[18] W. Stambouli, H. Elhouichet, M. Ferid, Journal of Molecular Structure **1028**, 39 (2012).
[19] R. A H. El-mallawany, Tellurite glasses handbook. 2002.
[20] S. Suehara, K. Yamamoto, S. Hishita, T. Aizawa, S. Inoue, **51(**21), 919 (1995).
[21] M. A. Villegas, J. M. F. Navarro, Journal of the European Ceramic Society, **27**(7), 2715 (2007).
[22] A. Kaur, A. Khanna, C. Pesquera, F. González, V. Sathe, Journal of Non-Crystalline Solids, **356**(18–19), 864 (2010).
[23] K. M. Kaky, G. Lakshminarayana, S. O. Baki, I. V. Kityk, Y. H. Taufiq-Yap, M. A. Mahdi, Results in Physics **7**, 166 (2017).
[24] E. Pavai, "RESEARCH ARTICLE ULTRASONIC AND STRUCTURAL PROPERTIES OF SiO 2 -PbO-Li 2 O GLASSES," **3**, 936 (2012).
[25] K. Sathish, S. Thirumaran, K. Sathish, S. Thirumaran, Spectrochimica Acta - Part A: Molecular and Biomolecular Spectroscopy **147(**10), 163 (2015).
[26] K. Lane, "2 . Crystalline phases of the C o - P - O system," **72,** 81 (1985).
[27] R. El-Mallawany, N. El-Khoshkhany, H. Afifi, Materials Chemistry and Physics **95**(2), 321 (2006).
[28] U. B. Chanshetti, V. A. Shelke, S. M. Jadhav, S. G. Shankarwar, T. K. Chondhekar, A. G. Shankarwar, V. Sudarsan, M. S. Jogad, Facta universitatis - series: Physics, Chemistry and Technology **9(**1), 29 (2011).
[29] A. A. El-moneim, Materials Chemistry and Physics, **173**, 372 (2016).
[30] S. Thirumaran, N. Karthikeyan, Journal of Ceramics, **2013**, 1 (2013).
[31] R. El-Mallawany, M. S. Gaafar, N. Veeraiah, Chalcogenide Letters, **12(**2), 67 (2015).
[32] R. El-Mallawany, Materials Chemistry and Physics **53**(2), 93 (1998).
[33] S. Inaba, S. Fujino, K. Morinaga, J. Am. Ceram. Soc., **82**, 3501 (1999).
[34] G. A. S. B. Bridge, R.A. El-Mallawany, E.F. Lambson, "The Elastic Behaviour Of TeO2 Glass Under Uniaxial And Hydrostatic Pressure," **69**, 117 (1984).